Article:
Silavwe, E, Somjit, N and Robertson, ID (2016) A Microfluidic-Integrated SIW Lab-on-Substrate Sensor for Microliter Liquid Characterization. IEEE Sensors Journal, 16 (21). pp. 7628-7635. ISSN: 1530-437X

https://doi.org/10.1109/JSEN.2016.2599099

A Microfluidic-Integrated SIW Lab-on-Substrate Sensor for Microliter Liquid Characterization

Evans Silavwe, *Student Member, IEEE*, Nutapong Somjit, *Member, IEEE* and Ian D. Robertson, *Fellow, IEEE*

***Abstract*— A novel microfluidic-integrated microwave sensor with potential application in microliter-volume biological/biomedical liquid sample characterization and quantification is presented in this paper. The sensor is designed based on the resonance method, providing the best sensing accuracy, and implemented by using a substrate-integrated-waveguide (SIW) structure combining with a rectangular slot antenna operating at 10 GHz. The device can perform accurate characterization of various liquid materials from very low to high loss, demonstrated by measurement of deionized (DI) water and methanol liquid mixtures. The measured relative permittivity, which is the real part of complex permittivity, ranges from 8.58 to 66.12, which is simply limited by the choice of test materials available in our laboratory, not any other technical considerations of the sensor. The fabricated sensor prototype requires a very small liquid volume of less than 7 μl, while still offering an overall accuracy of better than 3 %, as compared to the commercial and other published works. Key advantages of the proposed sensor are that it combines 1.) a very low-profile planar and miniaturized structure sensing microliter liquid volume; 2.) ease of design and fabrication, which makes it cost-effective to manufacture and 3.) noninvasive and contactless measurements. Moreover, since the microfluidic subsystem can potentially be detached from the SIW microwave sensor and, afterward, replaced by a new microfluidic component, the sensor can be reused with no life-cycle limitation and without degrading any figure of merit.**

***Index Terms* — Biological, permittivity measurements, resonance, slot antenna, SIW.**

I. Introduction

RESONANCE methods are the most accurate in liquid material detection and quantification compared to the other available alternatives such as transmission-line techniques [1]-[5]. The resonance methods are normally used to characterize materials at either a single frequency or a narrow band. Previously, resonance methods were restricted to measurement of low loss materials due to broadening of the resonance curve as the loss increased. However, the methods have recently been adapted to measure and characterize high-loss liquids through various modeling techniques [6]. Due to the high sensitivity of resonance methods, they particularly allow for reduction of sample volume and enhance sensor compactness [7].

With the advancement of substrate integrated waveguides (SIWs) in the last decade, it is now possible to design planar devices offering functionality for what was previously reserved for traditional waveguides. This reduces cost, offers reduced size and makes for easy integration with other planar circuits [8], [9]. Recently, in [10], an SIW resonator sensor for liquid permittivity measurements was presented. However, the sensor requires substantial liquid volume as well as sensor immersion in liquid. The immersion exposes the sensor to possibilities of contamination as well as corrosion. In [2] a planar resonator is presented, although compact, it is only able to characterize liquids with relative permittivity extending from 20 to 40 as these are the limits of the predictive model employed.

In this paper, we present a novel liquid sensor with application for liquid mixture solutions detection, identification and quantification, e.g. cell quantification, that combines the following advantages compared to the state-of-the-art: 1) measurement of relative permittivity, real part of complex permittivity, with ε'_r ranging from low ε'_r to high ε'_r materials with no technical restriction, 2) noninvasive and contactless characterization, 3) compact liquid volume, with only 7 μl being sufficient, and 4) potentially reusable sensor requiring only a replacement of the microfluidic subsystem in the plug-and-play fashion. The sensor is made reusable by creating guiding holes on the microfluidic subsystem and the microwave subsystem. Furthermore, a mathematical model is developed to analyze and synthesize the SIW sensor. Based on the proposed analytical model, a program implemented by using MATLAB is developed to transform the measured return losses and resonant frequencies to various interesting liquid material properties, e.g. dielectric constants. In [11], the authors presented the basic sensor structure with preliminary measurement results. In this paper, intensive design study, in-depth measurement results and performance comparisons as well as mathematical modeling are introduced for the first time. The frequency choice of 10 GHz is a compromise between sensor sensitivity and cost. At much lower frequency, the sensor would become less sensitive, while at very high frequency the sensitivity would increase but so would the fabrication cost and measurement challenge.

This work was supported by the Commonwealth Scholarship Commission.

The authors are with the Institute of Microwave and Photonics, School of Electronics and Electrical Engineering, University of Leeds, UK, (e-mails: el07es@leeds.ac.uk, n.somjit@leeds.ac.uk, i.d.robertson@leeds.ac.uk). An earlier version of this paper was presented at the European Microwave Conference 2016 and was published in its Proceedings.

II. WORKING PRINCIPLE AND SENSOR DESIGN

Figure 1 and Table I show the 3D structure and important design parameters of the SIW microfluidic-microwave sensor. The sensor is implemented using an SIW structure integrated on top with a longitudinal slot antenna, designed to operate at the center frequency of 10 GHz. The SIW is implemented based on a RT/Duroid 5880 substrate that is copper plated on the top and the bottom surfaces. Vertical copper plated via holes electrically connect the top copper layer to the bottom copper layer, thereby forming both side walls of the SIW. One edge of the SIW, as shown in Fig. 1, is short-circuited by using a series of vertical copper plated via interconnections. A longitudinal rectangular slot cavity antenna is then created into the top metallic layer with its center position located at a quarter-wavelength distance from the short-circuited end of the SIW. For the measurement, an additional 50-Ω microstrip feed line is integrated to the design with a tapered microstrip transition that matches the SIW impedance of 72-Ω to that of the 50-ohm microstrip. Electromagnetic (EM) field radiation from the rectangular slot antenna occurs because the slot cavity interrupts the transverse surface currents in the metallic wall of the SIW, thereby creating an electric field in the slot. The induced electric field can be viewed using its equivalent magnetic sheet and radiates into the outer space [12]. To create a contactless sensor, a dielectric layer is used to cover on top of the SIW slot antenna, acting as an isolation layer between microwave and microfluidic subsystems. A micro-fluidic subsystem, consisting of a micro-channel and liquid in and outlets, is then created in another substrate, which is subsequently bonded on top of the isolation layer. The final substrate layer, performing as a liquid-channel cover, was then bonded on top of the microfluidic subsystem to encapsulate the liquid inside the microfluidic channel. The microfluidic channel is transversely located above the center of the antenna slot where the radiated EM near-field is maximum in order to get the best sensing accuracy and sensitivity. The sensing principle is to track any changes in resonant frequency and return loss of the slot antenna as a result of an interaction between the radiated near-field and the encapsulated liquid in the micro-fluidic channel.

The SIW design procedure follows the steps given in [13]. The important design consideration is that the pitch (p) is less than or equal to twice the vias post diameter (d) and that the post diameter is less than a fifth of the guided wavelength (λ_g) as given in (1). Under this condition the field leakage can be negligible and the performance of the SIW structure is similar to the conventional rectangular waveguide. The SIW width (a_{SIW}) is then the equivalent dielectric waveguide width (a_e) given by (2), where a_{RWG} is the width of a conventional rectangular waveguide and ε_r is the relative permittivity of the substrate.

$$d < \frac{\lambda_g}{5} \text{ and } p \leq 2d \tag{1}$$

$$a_{SIW} = \frac{a_{RWG}}{\sqrt{\varepsilon_r}} \tag{2}$$

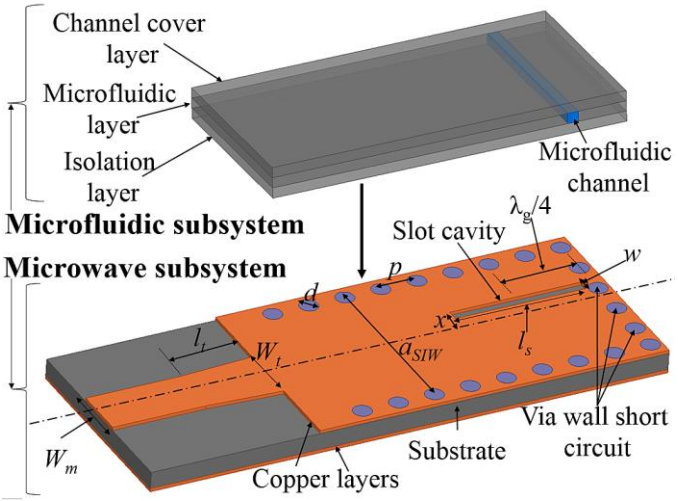

Fig. 1. 3D drawing of SIW waveguide integrated with a single slot antenna and microfluidic subsystem.

TABLE I
SUMMARY OF THE DESIGN PARAMETERS

Parameter	Description	Length (mm)
d	Via post diameter	0.5
p	pitch	0.8
a_{SIW}	SIW width	15.4
b	SIW height	1.575
l_s	Slot length	11.7
w	Slot width	0.5
x	Displacement from centre of SIW to centre of slot	1.85
l_t	Microstrip taper length	6.7
W_t	Microstrip taper width	5.4
W_m	50-Ω microstrip width	4.62

The Rogers RT/Duroid 5880 substrate used in implementing the SIW structure has a dielectric constant of 2.2 and a loss tangent of 0.0009 at 10 GHz. RT/Duroid 5880 has low moisture absorption, very good chemical resistance and offers the lowest electrical loss for reinforced Polytetrafluoroethylene (PTFE) material making it a good substrate for the dielectric encapsulating the liquid [14]. The optimum design parameters of the SIW waveguide are summarized in Fig. 1.

A single slot antenna is well sufficient to achieve highly accurate tracking of the resonant frequency changes and the return loss variations when different types of liquid samples are encapsulated in the channel above the antenna slot. The slot length (l_s) and the slot displacement from the SIW center (x) in Fig. 1 are optimized to obtain the lowest voltage standing wave ratio (VSWR). The displacement of the slot from the center of the SIW plays a critical role in the design, since it directly impacts on the effective resonant slot conductance. The displacement is calculated by using the Stevenson formula [15] that gives the effective resonant slot conductance.

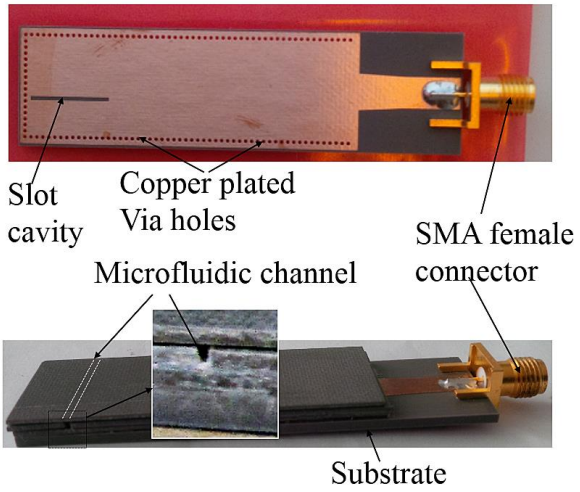

Fig.2 Fabricated prototype, before (top) and after (bottom) mounting the microfluidic subsystem.

$$g(x) = g_o Sin^2\left(\frac{\pi x}{a_{SIW}}\right) \quad (3)$$

$$g_o = (2.09 a_{SIW}\lambda_g / b\lambda_o) Cos^2(\lambda_o \pi / 2\lambda_g) \quad (4)$$

where $g(x)$ ($=G_s/G_{SIW}$) is the normalized conductance of a resonant longitudinal shunt slot, g_0 is a constant, λ_g is the guide wavelength, λ_0 is the free-space wavelength, x is the slot displacement from the center of the guide and a_{SIW} and b are the waveguide width and height [16]. G_s is the slot conductance and G_{SIW} is the guide characteristic conductance. The slot length (l_s) is impacted by the permittivity of the dielectric filling the waveguide. This was calculated by (5), [17].

$$l_s = \frac{\lambda_o}{\sqrt{2(\varepsilon_r+1)}} \quad (5)$$

For the design frequency of 10 GHz and substrate relative permittivity of 2.2, the calculated slot length is 11.86 mm. The parameter was further optimized with HFSS to 11.7 mm in order to achieve the lowest VSWR.

A tapered microstrip transition from a 50-Ω input microstrip line to the SIW was designed to achieve good matching over the whole operation band of the SIW [18]. The tapered microstrip line converts the TEM propagation mode of the microstrip to the TE_{10}, which is the fundamental mode, in the SIW.

The position of the microfluidic channel is determined based on the design rule that the radiated EM near-field is maximum at the quarter-wavelength distance from the short-circuited end of the SIW. In this design, the microfluidic channel is located at 6.7 mm from the short-circuited end of the SIW, in order to achieve the best sensing accuracy. The microfluidic subsystem is made up of three layers, the isolation layer, the microfluidic layer and the channel cover layer. All layers are precisely cut out using the LPKF 200 Protolaser machine in our laboratory. The three layers are aligned as shown in fig.3 for bonding. To ensure that the slot cavity is not in physical contact with the liquid sample

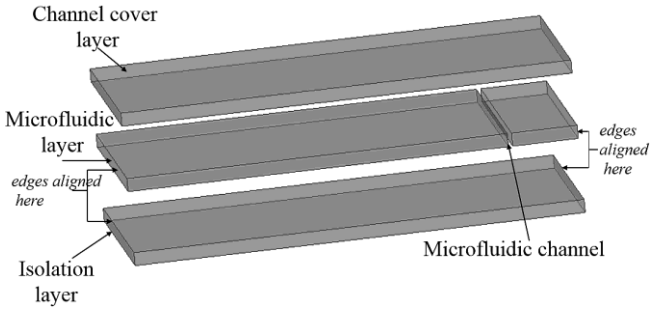

Fig.3 Precisely cut Microfluidic subsystem layers aligned at the edges.

under test, the isolation layer consisting of a low-loss dielectric substrate is bonded on top to cover the SIW antenna slot. The thickness of the isolation layer is 790 μm. However, adding a dielectric isolation layer on top of the slot results in a slight resonant frequency shift [19]: in this design from 10 GHz to 9.6 GHz. After integrating the isolation layer, the microfluidic subsystem is implemented on top by using another dielectric substrate containing a micro-channel. The height of the microfluidic channel is 790 μm, which equals the thickness of the substrate. Another dielectric substrate is then bonded on top to cover the microfluidic channel, ensuring the liquid is well encapsulated inside the microchannel. Epoxy bonding was used for all three substrate layers. All three dielectric substrates forming the microfluidic subsystem are implemented by using Rogers Duroid 5880. The width of the microfluidic channel is optimized by HFSS to 500 μm for the best sensing accuracy and sensitivity.

Fig. 2 shows the fabricated sensor prototype before (top) and after (bottom) integrating the microfluidic subsystem to the microwave SIW sensor, respectively.

III. MODEL ANALYSIS

An equivalent circuit model for the radiating area of the slot antenna was developed as shown in Fig. 4. It is developed by considering that because the slot interrupts the transverse currents of the SIW, the EM-wave radiation is induced from the slot both in the upward direction into the isolation layer and microfluidic channel as well as in the downward direction into the SIW. Fundamentally, if we can find the impedance or admittance attributed to the measured liquid, we can also accurately determine the relative permittivity of the liquid under test at the resonant frequency.

This becomes clear when it is considered that the slot cavity represents a rectangular waveguide. Similarly, the isolation, microfluidic and channel cover layers can be seen as dielectric waveguide slabs. The material properties of the unpatterned isolation and channel cover layers is sufficiently provided by the manufacturer, i.e. the Rogers Duroid 5880. The microfluidic layer, on the other hand, is composed of a micro-fluidic channel, filled with the liquid under test, embedded into the Rogers Duroid 5880 substrate. This means that only the permittivity of the liquid under test is unknown and must be determined. Understanding this enables the relative permittivity of the liquid to be calculated using transmission line analysis of

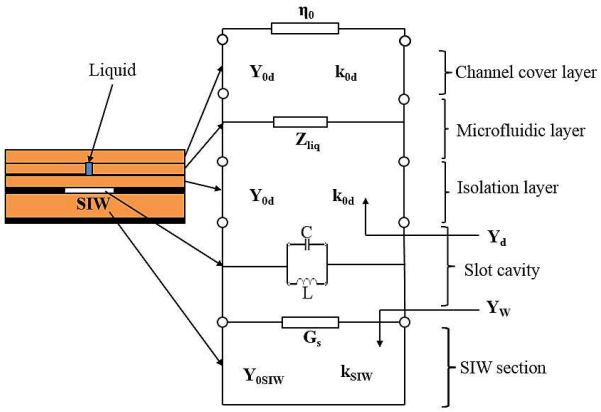

Fig. 4 SIW Sensor radiating area equivalent 2-D circuit

the conductance of the whole equivalent two-dimensional circuit model in Fig. 4, in relation to the measured resonant frequency and return loss.

The total conductance (G_t) of the equivalent circuit can be calculated as in [19] by

$$G_t = Y_w + Y_d + G_s + j\left(\omega C - \frac{1}{\omega L}\right) \tag{6}$$

where G_t is the total conductance of the entire equivalent model, G_s is the resonant conductance due to the thin slot, with C and L being capacitance and inductance of the slot cavity. Y_w and Y_d are respectively the admittance seen from the slot looking into the SIW and also from the slot looking into the isolation layer. This implies that Y_d is the effective admittance due to the isolation layer, the microfluidic layer and the liquid channel cover layer.

Resonance occurs when the slot admittance presented to the SIW is real [15]. In [19] it was investigated that the conductor wall thickness introduces a resonant frequency shift but leaves the resonant conductance of the antenna slot unaffected. The total conductance of the equivalent circuit can therefore be reduced to (7) at the resonance while still giving accurate results.

$$G_r = Y_w + Y_d + G_s \tag{7}$$

where G_r is the resonant conductance of the entire equivalent model. The slot resonant admittance, G_s, has already been defined in (3) and (4).

Assuming that the standing wave for the electric field across the slot is symmetrical, the return loss at the input port can be represented in the form of the equivalent shunt admittance (G_r/Y_{SIW}) as a result of the longitudinal slot in the broad wall of the waveguide [20].

$$S11c = \frac{-\frac{G_r}{Y_{SIW}}}{2+\frac{G_r}{Y_{SIW}}} \tag{8}$$

where Y_{SIW} is the characteristic admittance of the waveguide, which, in this case, is the equivalent characteristic admittance of the SIW, tapered transition and the 50-Ω microstrip. S_{11c} is the calculated reflection coefficient at the input port. The expressions of the impedance variables in Fig. 4 were developed as follows. From transmission line theory,

$$Y_w = -jY_{0SIW}cot(k_{SIW}b) \tag{9}$$

where the characteristic admittance in the guide below the slot is given by

$$Y_{0SIW} = \frac{\beta_d}{k_0\eta_0} \tag{10}$$

and $k_{SIW} = \frac{2\pi\sqrt{\varepsilon_s}}{\lambda_o}$ with ε_s being the relative permittivity of the dielectric filling the SIW. β_d is the propagation constant in the dielectric given by

$$\beta_d = \sqrt{\varepsilon_s {k_0}^2 - \left(\frac{\pi}{l_s}\right)^2} \tag{11}$$

where l_s is the length of the slot cavity.

Y_d is equally calculated using the transmission line theory. This is done by considering the impedance due to the isolation layer and a combination of the microfluidic layer and the impedance due to the liquid channel cover layer.
Y_d can then be defined as

$$Y_d = Y_{0d}\frac{1+jZ_{eq}Y_{0d}\tan(k_{0d}h)}{Z_{eq}Y_{0d}+jtan(k_{0d}h)} \tag{12}$$

where Z_{eq} is the total impedance seen looking into the microfluidic layer from the isolation layer, given in (13) and Y_{0d} (which in this case is the same as Y_{0SIW}) is the characteristic admittance of the isolation layer and k_{0d} is equal to k_{SIW} since the dielectric used in both cases has similar properties.

$$Z_{eq} = Z_{liq}\frac{Z_{0d}+jZ_{liq}tan(k_{liq}h)}{Z_{liq}+jZ_{0d}\tan(k_{liq}h)} \tag{13}$$

where $Z_{liq}\left(=\frac{k_0\eta_0}{\beta_{liq}}\right)$ is the characteristic impedance due to the microfluidic layer, while k_{liq} $(=\frac{2\pi\sqrt{\varepsilon_{eff}}}{\lambda_o})$ is the propagation constant in the microfluidic layer. ε_{eff} is the effective permittivity, which is the permittivity as a result of the liquid under test and the dielectric forming the microfluidic channel given by Maxwell-Garnet relationship as

$$\frac{\varepsilon_{eff}-\varepsilon_{liq}}{\varepsilon_{eff}+2\varepsilon_{liq}} = f\frac{\varepsilon_s-\varepsilon_{liq}}{\varepsilon_s+2\varepsilon_{liq}} \tag{14}$$

where ε_{liq} and ε_s are the relative permittivity of the liquid and the dielectric forming the microfluidic channel respectively, while f is the fractional volume occupied by the dielectric in the microfluidic layer. The Maxwell-Garnet model was used because the electric field is considered constant across the mixture of the dielectric substrate and the liquid under test. The Maxwell-Garnet is also designed for small volume fractions of inclusions [21] and is easy to solve.

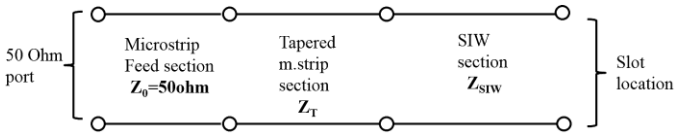

Fig. 5 Equivalent model of the feed network.

To calculate the characteristic impedance of the waveguide feed network, the three sections of the feed network, consisting of the SIW, tapered microstrip transition and microstrip feedline, are considered as a cascade as shown in Fig. 5.

Each section of the feed network in Fig. 5 is designed using HFSS and their S-parameters are obtained. The S-parameters are converted to ABCD parameters so that the total ABCD parameters of the cascade can be obtained as

$$[T_{in}] = [T_m].[T_t].[T_{SIW}] \tag{15}$$

where $[T_{in}]$ represents the total cascade ABCD parameters of the feed circuit with $[T_m]$, $[T_t]$ and $[T_{SIW}]$ representing the ABDC parameters for the 50-Ω microstrip, the tapered microstrip and the SIW sections, respectively. The ABCD parameters for the entire feed network are then converted back to S-parameters and used to obtain the equivalent characteristic impedance of the whole feed structure as

$$Z_{SIW} = Z_0\sqrt{\frac{(1+S_{11})^2-S_{21}{}^2}{(1-S_{11})^2-S_{21}{}^2}} \tag{16}$$

Substituting (3), (9) and (12) in (7) and then using (8) and (16), an expression for S_{11c} can be written with the effective relative permittivity of the liquid and dielectric forming the microfluidic subsystem as a variable.

The calculated S_{11c} is then iteratively compared with the measured S_{11m} to get the effective relative permittivity of the liquid and dielectric sample holder as in (17a) and (17b). In this particular case, the solve system, fsolve, of nonlinear equations in MATLAB was used, together with the MATLAB program developed by the authors, to numerically calculate the effective relative permittivity of the liquid at the resonant frequency. The known relative permittivity of the dielectric material forming the microfluidic subsystem was used as the initial value. Therefore, the relative permittivity of the liquid under test can be numerically calculated at the resonant frequency of the measurement using (14). The relative permittivity of various liquids and liquid mixtures characterized by the SIW sensor is compared to that measured by the KeySight 85070E dielectric probe sensor [22], under the same environment control. The measurement result comparisons are shown in the results section.

$$f(\varepsilon_{eff}) = Re(S_{11m} - S_{11c}) \tag{17a}$$
$$f(\varepsilon_{eff}) = Im(S_{11m} - S_{11c}) \tag{17b}$$

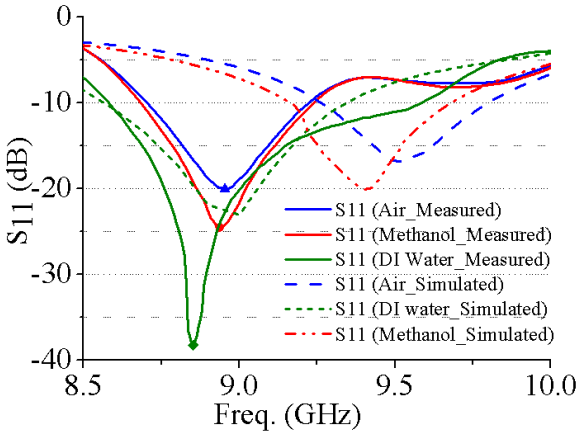

Fig. 6 S_{11} plot for simulated and measured Air, Methanol and DI water samples.

IV. MEASUREMENT RESULTS

A. Measurement setup, sensor calibration and basic measurement

The liquid under test is, prior to each measurement, injected into the microfluidic channel using a 100 μl syringe with one end of the microfluidic channel well capped. The liquid is let to overflow at the inlet before the microchannel inlet is capped to ensure complete liquid filling. When the microchannel is completely filled by the liquid under test without any air gap or bubble, the liquid inlet of the microchannel is then sealed. The S-parameter measurement is done by using the Keysight E8361A Network Analyzer. One-Port reflection calibration was done using the Keysight Electronic Calibration (ECal) N4691-60006 module prior to the measurement. All liquids were maintained at 25°C by using a warm water beaker that was maintained at 25°C.

Three sample materials, which are air, Methanol and DI water, were measured and characterized. Air is measured in order to calibrate the measurement for an empty microfluidic channel, while the other two materials had their respective liquids filled in the channel.

Fig. 6 shows that with the empty, air-filled, microfluidic channel, the measured resonant frequency of the SIW sensor was 8.96 GHz with a return loss of 20.02 dB. With methanol and DI water samples, the resonant frequency was 8.94 GHz with a return loss of 24.51 dB and 8.85 GHz with a return loss of 38.21 dB, respectively. A resonant frequency shift of 110 MHz was observed between DI water and air (empty channel), while a shift of 20 MHz was observed between methanol and air.

The resonant frequency shifts between the empty channel and liquid-filled channel are significant and; therefore, it is clear that well accurate characterizations and discriminations between each different liquid material under test can be obtained.

For all simulations, HFSS used the default meshing setting with the lambda target set at 0.3333. HFSS then used auto-adaptive meshing based on the fields for it to obtain the final mesh. Fig. 6 shows that the simulated results are shifted in

frequency and return loss because the epoxy effect was not included, difference in conductor loss used, and also the simulation uses approximated properties for the samples under test. The measured values are used for subsequent calculations.

B. Quantification Measurement of liquid mixture

The SIW sensor demonstrated liquid quantification by measuring liquid mixtures of DI water and methanol with methanol to DI water composition varying from 0-100 % by volume. An increment of methanol volume by 20 % corresponding to an equal decrease of DI water by volume for each measurement step was conducted. Zero percent methanol constituent in the liquid mixture indicated 100 % DI water. Fig. 7 shows the measurement result indicating the reflection coefficient (S_{11}) of the different liquid mixtures.

Varying mixture concentration gives an equivalent change in resonant frequency and return loss. This change is mostly because a high loss liquid has more perturbation effect on the radiated near-field than a lower loss liquid and hence having a lower resonant frequency. Therefore, by starting with 100 % methanol and decrement each measurement step downwards by 20 % by volume, it was observed that the resonant frequency correspondingly shifted downwards as more water by volume dominated the test sample.

This is illustrated in Table II and Fig. 8, with values for the mixture characterization model, developed by a fitting curve method, included. This characterization model therefore embodies the behavior of this particular mixture and can be subsequently be used to determine the composition of any given DI water – methanol mixture.

The equation characterizing the mixture measurement is given as

$$V_f = 1.47x10^4 f_r{}^4 - 5.22x10^5 f_r{}^3 + 6.94x10^6 f_r{}^2 - 4.1x10^7 f_r + 9.1x10^7 \quad (18)$$

Where V_f is the fractional volume of methanol and f_r is the measured resonant frequency.

C. Relative permittivity measurement

Using the software program developed from the mathematical model in section III, it is possible to determine the relative permittivity (real part of the complex permittivity) of the liquid under test. This was achieved by solving iteratively the equations given in (17a) and (17b). The relative permittivity was calculated for the DI water and methanol mixtures mentioned in the preceding subsection. These liquids and liquid mixtures were also measured using the Keysight 85070E dielectric probe under the same environment control and condition. As shown in Table III, the results showed good agreement between the SIW sensor and the commercial probe, with the percentage difference between the two sensor devices varying from 0.4 % to 3 %. However, for the SIW sensor, only 7 μl of the sample liquid is required for an accurate measurement while the commercial probe requires more than 100ml for the same accuracy. In Table IV, key figure-of-merit and parameter comparisons between this work and the state-of-the-art [2] and [23]-[25] are presented.

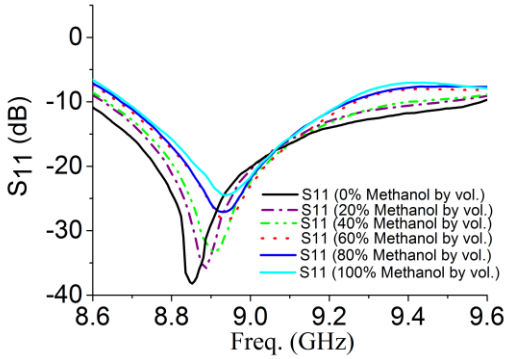

Fig. 7 Measured S_{11} plot for Methanol and DI water mixtures.

TABLE II
DEIONISED WATER-METHANOL MIXTURE MEASUREMENT

Frequency (GHz)	Methanol fractional volume (measured)	Methanol fractional volume (Model)	Percentage difference
8.86	0	0.00067215	0
8.88	0.2	0.20378764	1.89382
8.90	0.4	0.39054383	2.364042
8.92	0.6	0.61892344	3.153907
8.93	0.8	0.78270568	2.16179
8.94	1.0	1.0047337	0.47337

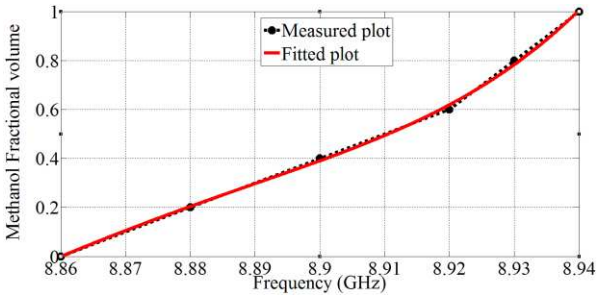

Fig.8 Methanol fractional volume against resonant frequency.

TABLE III
RELATIVE PERMITTIVITY MEASUREMENT OF METHANOL/DI WATER MIXTURE USING SIW SLOT ANTENNA AND THE KEYSIGHT DIELECTRIC PROBE

Test sample (by volume)	Freq. (GHz)	Relative Permittivity (this work)	*Relative permittivity (Keysight probe)	% diff.
100%Methanol	8.94	8.58	8.37	2.44
80% Methanol	8.93	11.92	11.63	2.43
60% Methanol	8.92	23.55	22.86	2.93
40% Methanol	8.90	34.54	34.39	0.43
20% Methanol	8.88	48.67	48.44	0.47
100% DI water (0% methanol)	8.85	66.12	65.67	0.68

*Measured using Keysight 85070E probe sensor.

Simulations were performed to analyse the sensitivity of the sensor. Three test samples with relative permittivity of 10,

10.01 and 10.1 were used, low ε'_r values are used here to prove good sensitivity for low relative permittivity liquids. The sensitivity of the sensor can be approximated to be ±0.1 ε'_r.

V. CONCLUSION

The developed microwave microliter sensor in this work has shown some of its potential range of usage leading to accurate quantification of liquid mixtures and further liquid characterization through measurement of the relative permittivity. The accuracy in measurement was enhanced by the resonance operation of the sensor. This ensured that with only 7 μl of the liquid, sufficiently accurate results were obtained. Furthermore, the developed model based on a dielectric covered waveguide fed slot antenna enhanced confidence in the obtained results. The quantification measurements of DI water and Methanol mixtures with methanol varying in increments of 20 % by volume gave a good indication of how this sensor could be applied. Equally the measured relative permittivity of the liquids affirmed the universal nature of the characterization range, therefore lending this sensor to potentially vast applications. This microwave microliter sensor consequently has potential in the characterization of biological liquids.

TABLE IV
KEY PARAMETER COMPARISON OF MEASUREMENT OF THIS WORK AND OTHERWORK

Key Parameter	[2]	[22]	[23]	[24]	[25]	This work
Relative permittivity (ε'_r) of deionised water	Reported only S_{21} results	65.67	63	63.5	66.5	66.12
Liquid volume	*nl*	100 *ml*	1.8 *ml*	1.16 *ml*	Not indicated	7 μl
Freq. for DI water measurement (GHz)	17.9-19.34	8.85	9.7	9.7	8.5	8.5
Fabrication complexity	Moderate	Moderate	Moderate	Moderate	N/A**	Low
Lab-on-substrate suitability	Yes	No	No	No	N/A	Yes
Characterisation method	Resonance	Reflection	Transmission	Transmission	N/A	Resonance
Permittivity measurement range	20 – 40*	Not limited	Not limited	Not limited	Not limited	Not limited
Planar structure	Planar	Non-planar	Non-planar	Non-planar	N/A	Planar
Measurement setup	Non-invasive and contactless	Non-invasive	Non-invasive	Non-invasive	N/A	Non-invasive and contactless
Fabrication	Cleanroom	Standard machining	Standard machining	Standard machining	N/A	Standard PCB
Design complexity	Complicated	Moderate	Moderate	Moderate	N/A	Moderate

*Limited to indicated range because of the predictive model.
**Results obtained using developed interpolation function.

REFERENCES

[1] G. Gennarelli, S. Romeo, M.R. Scarfì, F. Soldovieri, "A microwave resonant sensor for concentration measurements of liquid solutions," *IEEE Sensors Journal,* vol. 13, pp. 1857 - 1864, May 2013.

[2] T. Chretiennot, D Dubuc, K. Grenier, "A microwave and microfluidic planar resonator for efficient and accurate complex permittivity characterisation of aqueous solutions," *IEEE Trans. Microw. Theory and Techniques*, vol. 61, no. 2, pp. 972-978, February 2013.

[3] A.H. Sklavounos, N.S. Barker, "Liquid-permittivity measurements using a rigorously modeled overmoded cavity resonator," IEEE *Trans. On Microwave Theory and Techniques*, vol. 62, no. 6, pp. 1363-1372, June 2014.

[4] A.I. Gubin, A.A. Barannik, N.T. Cherpak, I.A. Protsenko, S. Pud, A. Offenhausser, S.A. Vituserich, "Whispering-gallery-mode technique with microfluidic channel permittivity measurement of liquid," *IEEE Trans. Microw. Theory and Tech.*, vol. 63, no. 6, pp. 2003-2009, June 2015.

[5] H. Lobato-Morales, A. Colona-Chavez, J.L. Olvera-Cervantes, R.A. Chavez-Perez, J.L. Medina-Monroy, "Wireless sensing of complex dielectric permittivity of liquids based on the RFID," *IEEE Trans. Microw. Theory and Tech.*, vol. 62, no.9, pp. 2160-2167, September 2014.

[6] H. Kawabata, H. Tanpo, Y. Kobayashi, "A rigorous analysis of a TM_{010} mode cylindrical cavity to measure accurate complex permittivity of liquid," *33rd Eur. Microw. Conf.*, pp. 759–762, 2003.

[7] S. Liu, I. Ocket, B. Nauwelaers, W. De Raedt, "A 60GHz liquid sensing substrate integrated cavity in LTCC," *43rd Eur. Microw. Conf.*, pp. 613-615, October 2013.

[8] C. Shi, H. Yousef and H. Kratz, "79GHz slot antennas based on substrate integrated waveguides (SIW) in a flexible printed circuit board," *IEEE Trans. on Antenna and Propagation.,* vol. 57, no. 1, pp. 64-71, January 2009.

[9] M. Henry, C.E. Free, B.S. Izqueirdo, J. Batchelor, "Millimetre wave substrate integrated waveguide antennas: design and fabrication analysis," *IEEE Trans. on Advanced Packaging,* vol. 32, pp. 93-100, February 2009.
[10] C. Liu, F. Tong, "An SIW resonator sensor for liquid permittivity measurements at C Band," *IEEE Microw. . Wirel. Comp. Lett.,* vol. 25, pp 751–753, Nov. 2015.
[11] E. Silavwe, N. Somjit, I.D. Robertson, "Microwave microlitre lab-on-substrate liquid characterisation based on SIW slot antenna," *European Microw. Conf.,* October, 2016 (Accepted).
[12] R.S. Eliiot, Antenna Theory and Design, Revised Edition, John Wiley & Sons, New York, 2003.
[13] D. Deslandes, K. Wu, "Single-substrate integration technique of planar circuits and waveguide filters," *IEEE Trans. on Micro. Theory and Tech.,* vol. 51, no. 2, pp. 593-596, Feb. 2003.
[14] Rogers Corporation, RT/duroid 5880 datasheet, https://www.rogerscorp.com/documents/606/acs/RT-duroid-5870-5880-Data-Sheet.pdf.
[15] S. Silver, *Microwave Antenna Theory and Design*, London: Peter Peregrinus, 1986.
[16] R.C. Johnson, Antenna Engineering Handbook, McGraw-Hill Inc, Third Edition, 1993.
[17] A.J. Farrall, and P.R. Young, "Integrated waveguide slot antennas," *Elect. Lett.,* vol. 40, no.16, Aug. 2004.
[18] D. Deslandes, "Design equations for tapered microstrip-to-substrate integrated waveguide transitions," *IEEE MTT 2010 International Microwave Symposium.*
[19] P.B. Katehi, "Dielectric-covered waveguide longitudinal slots with finite wall thickness," *IEEE Trans. on Antennas and Propagation,* vol. 38, no. 7, pp. 1039-1045, July 1990.
[20] N. Amiri, K. Forooraghi, "Analysis of a dielectric-covered waveguide slot antenna using the spectrum of two-dimensional solutions," *IEEE Transactions on Antenna and Propagation,* vol. 62, no. 7, pp. 3818-3823, July 2014.
[21] L. Jylha, A. Sihvola, "Equation for the effective permittivity of particle-filled composites for material design applications," *Journal of Physics D: Applied Physics,* vol. 40, pp. 4966-4973, 2007.
[22] Keysight Technologies, Technical Overview, http://literature.cdn.keysight.com/litweb/pdf/5989-0222EN.pdf?id=364444.
[23] U.C. Hasar, J.J. Barroso, Y. Kaya, M. Ertugrul, M. Bute, "Reference-plane invariant transmission-reflection method for measurement of constitutive parameters of liquid materials," *Sensors and Actuators A: Physical,* 203 (2013), pp. 346-354.
[24] U.C. Hasar, "A microwave method for noniterative constitutive determination of thin low-loss or lossy materials," *IEEE Transactions on Microwave Theory and Techniques,* vol. 57, no. 6, pp. 1595-1601, June 2009.
[25] W.J. Ellison, "Permittivity of pure water, at standard atmospheric pressure, over the frequency range 0-25THz, and the temperature range 0-100°C," *J. Phys. Chem., Ref. Data*, vol. 36, no. 1, pp. 1-18, February 2007.

Evans Silavwe (SM'14) received his MSc in Communications Engineering in 2008 from the University of Leeds and B.Eng in 2001 from the University of Zambia. He is currently working towards the Ph.D. degree in the Institute of Microwave and Photonics at the University of Leeds. His research interests include development of microwave microfluidic sensors and millimetre wave substrate integrated circuit applications.

Nutapong Somjit (M'10) received the Dipl.-Ing. (MSc) degree from Dresden University of Technology in 2005 and the PhD degree from the KTH Royal Institute of Technology in 2012. Then, he returned to Dresden to lead a research team in micro-sensors and MEMS ICs for the Chair for Circuit Design and Network Theory. In 2013, he was appointed Lecturer (Assistant Professor) in the School of Electronic and Electrical Engineering, University of Leeds. His main research focuses on RFICs, RF MEMS, tuneable antennas, and RFIC-MEMS integration. Dr Somjit was the recipient of the Best Paper Award (EuMIC prize) at the European Microwave Week in 2009. He was awarded a Graduate Fellowship from the IEEE Microwave Theory and Techniques Society (MTT-S) in 2010 and 2011, and the IEEE Doctoral Research Award from the IEEE Antennas and Propagation Society in 2012. In 2016, he was the Chair of the Student Design Competition for the European Microwave Week.

Ian D. Robertson, (F'12) received his BSc (Eng.) and PhD degrees from King's College London in 1984 and 1990, respectively. From 1984 to 1986 he worked in the GaAs MMIC Research Group at Plessey Research, Caswell. After that he returned to King's College, initially as a Research Assistant working on the T-SAT project and then as a Lecturer, leading the MMIC Research Team and becoming Reader in 1994. In 1998 he was appointed Professor of Microwave Subsystems Engineering at the University of Surrey, where he established the Microwave Systems Research Group and was a founder member of the Advanced Technology Institute. In June 2004 he was appointed to the Centenary Chair in Microwave and Millimetre-Wave Circuits at the University of Leeds. He was Director of Learning and Teaching from 2006 to 2011 and Head of School from 2011 to 2016. He has 30 years of teaching experience in RF and microwave engineering and has published over 400 peer reviewed research papers. He edited the book MMIC Design published by the IEE in 1995 and co-edited the book RFIC & MMIC Design and Technology, published in English 2001 and in Chinese in 2007. He was elected Fellow of the IEEE in 2012 in recognition of his contributions to MMIC design techniques and millimetre-wave system-in-package technology. He was General Technical Programme Committee Chair for the European Microwave Week in 2011 and 2016.